Space- and Time-resolved Resistive Measurement of Liquid Metal Wall Thickness

S.M.H. Mirhoseini and F.A. Volpe[a)]
Dept of Applied Physics and Applied Mathematics, Columbia University, New York, NY 10027, USA

(Dated: 14 July 2016)

In a fusion reactor internally coated with liquid metal, it will be important to diagnose the thickness of the liquid at various locations in the vessel, as a function of time, and possibly respond to counteract undesired bulging or depletion. The electrical conductance between electrodes immersed in the liquid metal can be used as a simple proxy for the local thickness. Here a matrix of electrodes is shown to provide spatially and temporally resolved measurements of liquid metal thickness in the absence of plasma. First a theory is developed for $m \times n$ electrodes, and then it is experimentally demonstrated for 3×1 electrodes, as the liquid stands still or is agitated by means of a shaker. The experiments were carried out with Galinstan, but are easily extended to Lithium or other liquid metals.

PACS numbers: 52.35.Py,52.65.Kj,61.25.Mv,72.15.Cz

arXiv:1606.04008v2 [physics.plasm-ph] 13 Jul 2016

I. INTRODUCTION

Liquid metals (LMs) are attractive low-recycling plasma-facing materials[1–4] that could protect the underlying solid walls of a fusion reactor from high heat and neutron fluxes[5–7].

Lithium has been frequently used[1–4], but Tin, Lithium-Tin alloys, Gallium, the molten salt FliBe and other materials are also being considered[5–7]. These materials introduce new diagnostic requirements compared with confinement devices featuring solid walls. For example, CDX-U and LTX were equipped with spectrometers in the visible and extreme ultraviolet, with special attention paid to neutral Lithium, Li II and Li III lines[8,9].

An additional diagnostic requirement is posed by the very fact that these walls are liquid and thus can deform[10] under the effect of instabilities, turbulence, as a result of non-uniform force fields or currents from the plasma[11–14]. Deformations are undesired for various reasons[14], therefore they need to be monitored as a function of space and time, with resolutions of the order of a centimeter (in the poloidal and toroidal direction) and 10 ms[14].

The sensitivity and precision in the radial direction, on the other hand, are dictated by the two lengthscales that need to be monitored and preserved. These are the distance between the LM surface and the last closed flux surface (typically few cm) and the LM thickness. The thickness can range from sub-millimeter to meters, depending whether the LM is only used for its benign plasma-facing properties (low erosion, low recycling etc.) or is also meant to attenuate heat and neutrons. All things considered, millimeter precision is expected to suffice in most cases.

In a previous work[14] we had shown that, quite simply, and on the net of small corrections, the electrical conductance between two electrodes immersed in the LM scales linearly with the local LM thickness. Resistive measurements were used to infer the LM thickness in a single location and at a single time[14].

Here, after briefly describing the experimental setup (Sec.II), we extend the measurements to multiple locations, requiring matricial formalism (Sec.III), and to multiple times (Sec.IV).

II. EXPERIMENTAL SETUP

Here we recapitulate an earlier description of the setup[14] and report recent improvements.

The setup features a container filled for 5-25 mm with a low melting point (10°C) eutectic alloy of Gallium, Indium and Tin called Galinstan. This is about as good an electric conductor as Lithium (17% and 16% of copper, respectively).

Embedded in the container are 3×4 copper electrodes of 2 mm diameter and various lengths, for comparison (1, 16 and 25 mm, each with its own advantages and disadvantages[14]). Adjacent electrodes are spaced by 25 mm in one direction and 15 mm in the other.

The electrodes are connected to adjustable current-sources as well as to voltmeters referenced to ground. A shunt resistor is connected in series with the current-source, to measure the electrode current. As of recently, voltage and current signals are digitized at up to 10^5 KSa/s and digitally filtered from high-frequency noise (typically f <500 Hz). A LabView interface analyzes these data and returns the electrical resistance and LM thickness between each pair of electrodes, in real time (typically every 10-100 ms).

a)fvolpe@columbia.edu

III. SPACE-RESOLVED MEASUREMENTS

A. Theory

Consider $m \times n$ electrodes, evenly spaced in the x and y direction, at distances dx and dy, respectively, between adjacent electrodes. The electrodes are connected to individual power-supplies. These can inject or extract current in the LM, in the z direction orthogonal to the xy plane. However, no charge is accumulated, and $\nabla \cdot \mathbf{j}$=0. That is, Kirchhoff's law applies: the sum of all currents emitted or collected by an electrode is zero. The convention is adopted here that emitted currents are positive; collected currents are negative. In general, there are five such currents for each electrode: four in the xy plane, pointing at adjacent electrodes, and one in the z direction. Boundary or corner electrodes, on the other hand, only connect to three or two adjacent electrodes and one power supply.

Currents can obviously flow from or to *any* other electrode, not necessarily adjacent. Nonetheless, it is not necessary to model the system as a complicated network where all electrodes are directly connected to each other, forming a total of $mn(mn-1)/2$ connections. Instead, a Cartesian grid of $2mn - m - n$ resistors suffices. In this representation, each electrode is directly connected to only four adjacent electrodes via resistors, indicative of the LM thickness in between. Currents can flow from one electrode to another along several different routes on this Cartesian grid; the total resistance between two remote electrodes can be calculated by repetead application of simple sum rules for resistors in series or parallel. The total resistance between adjacent electrodes, on the other hand is, with good approximation, that of the very resistor that directly connects them.

Let us call $I_{i,j}$ the current emitted by electrode i,j and directed at the power supply. Let $V_{i,j}$ denote the potential of electrode i,j relative to some ground reference. The current emitted from electrode i,j to electrode $i,j+1$ will be proportional to the electric field $E_y = (V_{i,j+1} - V_{i,j})/dy$, to conductivity σ, and to the cross-sectional area $h_{i,j+1/2}dx$, where $h_{i,j+1/2}$ is the LM height in the midpoint between the two electrodes. After similar considerations for the other electrodes in the stencil, Kirchhoff's law writes:

$$\begin{aligned}\frac{I_{ij}}{\sigma} =& \frac{V_{i,j} - V_{i,j+1}}{dy} h_{i,j+\frac{1}{2}} dx + \frac{V_{i,j} - V_{i,j-1}}{dy} h_{i,j-\frac{1}{2}} dx \\ &+ \frac{V_{i,j} - V_{i+1,j}}{dx} h_{i+\frac{1}{2},j} dy + \frac{V_{i,j} - V_{i-1,j}}{dx} h_{i-\frac{1}{2},j} dy,\end{aligned} \tag{1}$$

except for boundaries and corners of the domain, where one or two terms drop from the right hand side. In this equation, σ is fixed by the material, dx and dy by the geometry, currents and voltages are measured, and the heights are the unknowns. The substitution $2/h_{i,j+\frac{1}{2}} = 1/h_{i,j} + 1/h_{i,j+1}$ and similar ones were omitted for brevity. Here the adoption of an harmonic mean instead of an arithmetic average is justified by the fact that the resistance between electrodes i,j and $i,j+1$ is the sum of the resistances of the layers in between, which are inversely proportional to the local heights. Also note that, by evaluating the heights in the mid-points between electrodes, rather than at the electrodes, there would be a total of $2mn - m - n$ unknown heights.

Eq.1 describes a set of mn equations in mn unknowns h_{ij}. The problem can be cast in matricial form $\mathbf{I} = \mathbf{A}\mathbf{h}$. Here $\mathbf{I}$ and $\mathbf{h}$ are one-dimensional arrays containing mn values of currents and heights, respectively. The block-diagonal matrix $\mathbf{A}$ is large, but features only five non-vanishing elements in each row (or four, or three, in rows corresponding to boundaries or corners), easily deduced from Eq.1. Ultimately we can solve for the LM heights by a simple matrix inversion, $\mathbf{h} = \mathbf{A}^{-1}\mathbf{I}$.

It should be noted that Ohm's law $\mathbf{j} = \sigma\mathbf{E}$ was used in Eq.1, instead of the more general $\mathbf{j} = \sigma(\mathbf{E} + \mathbf{v} \times \mathbf{B})$. This is legitimate under the assumptions that: (1) the liquid wall is thin and not significantly bulging or depleting ($v_z = 0$) and (2) there is no error field orthogonal to the wall (B_z =0). Under these assumptions, $\mathbf{v} \times \mathbf{B}$ has no x nor y components, hence it cannot perturb the currents between electrodes. An alternative requirement is that (3) the flow is slow enough that the x and y components of $\mathbf{v} \times \mathbf{B}$ are negligible compared with the corresponding components of $\mathbf{E}$. A realistic system violates these assumptions, and Eq.1 needs to be generalized:

$$\begin{aligned}\frac{I_{ij}}{\sigma} =& \left[\frac{V_{i,j} - V_{i,j+1}}{dy} + (v_x B_z - v_z B_x)_{i,j+\frac{1}{2}}\right] h_{i,j+\frac{1}{2}} dx \\ &+ \left[\frac{V_{i,j} - V_{i,j-1}}{dy} - (v_x B_z - v_z B_x)_{i,j-\frac{1}{2}}\right] h_{i,j-\frac{1}{2}} dx \\ &+ \left[\frac{V_{i,j} - V_{i+1,j}}{dx} + (v_z B_y - v_y B_z)_{i+\frac{1}{2},j}\right] h_{i+\frac{1}{2},j} dy \\ &+ \left[\frac{V_{i,j} - V_{i-1,j}}{dx} - (v_z B_y - v_y B_z)_{i-\frac{1}{2},j}\right] h_{i-\frac{1}{2},j} dy.\end{aligned} \tag{2}$$

This requires knowledge of the components of $\mathbf{v}$ and $\mathbf{B}$ in the midpoints between electrodes. Such knowledge could be provided by separate diagnostics, assumptions or calculations, or $\mathbf{v}$ and $\mathbf{B}$ might be reasonably fixed in the experiment. With this external input to matrix $\mathbf{A}$, the problem can be solved as a simple matrix inversion again, $\mathbf{h} = \mathbf{A}^{-1}\mathbf{I}$.

B. Experiment

Three 1 mm tall copper electrodes (one column of the 3×4 matrix) were used for space-resolved measurements. The DC current generator is connected to the first and the last electrodes in the row (Fig. 1). The LM thickness between electrodes E2 and E3 is varied by inserting a non-conducting cube in the space over and between these electrodes. Heights h_1 and h_2 were measured simultaneously by the resistive sensors, using Eq.1 for m=3 and

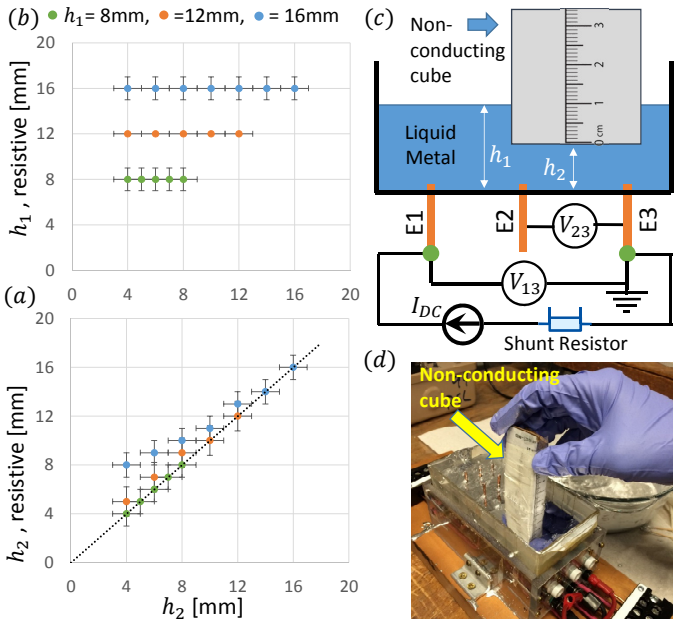

FIG. 1. Scheme of the space-resolved measurement test and the results; a) and b) h_2 and h_1 resistively measured versus h_2 measured by a Teflon coated ruler, c) scheme of the sensor, with the applied current and resistance measurement and d) experimental setup.

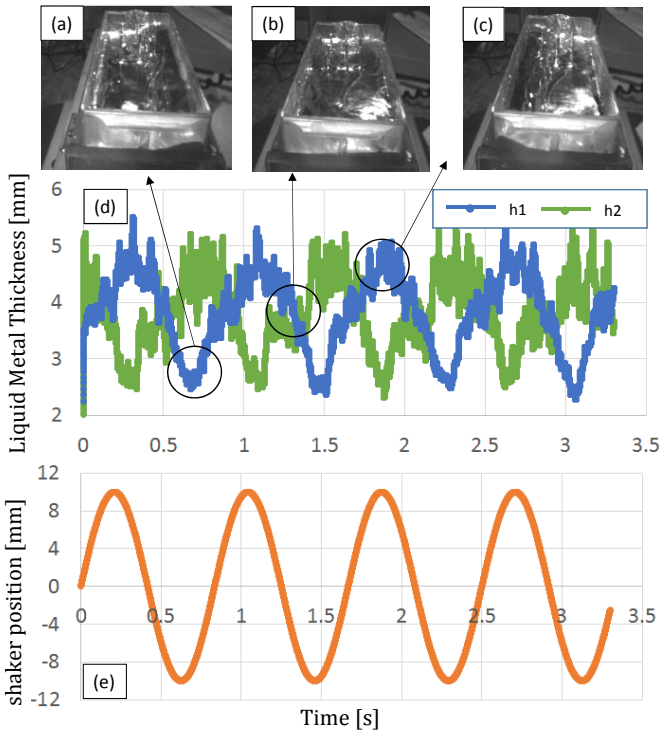

FIG. 2. Results of the space- and time-resolved measurements using a matrix of 3×1 copper, 1mm tall electrodes. The sensor container, including 4 mm deep of Galinstan is linearly moving in the horizontal direction at 72 RPM. a), b) and c) show the LM sensor at three different time steps corresponding to the points indicated on the measurement graph (d) and e) is the shaker position. h_1 and h_2 correspond to the heights measured by the left and right sensors.

n=1. The results are plotted in Fig. 1. The sensor is more accurate when measuring lower h_1 values. This is reasonable, since by increasing the LM height, the current between the short electrodes is not uniformly distributed, which decreases the accuracy of the theoretical model.

Another test was accomplished with the same setup, where this time the LM thickness was varied by tilting the entire LM pot. A difficulty was observed when resistively measuring the increase of h_1. The sensor was not able to follow the increase, while it was correctly measuring the decrease in h_2. The specular issue occurred when tilting to the opposite direction.

IV. TIME-RESOLVED MEASUREMENTS

Voltages at and currents between 3×1 electrodes were digitized at 10^5 kSa/s and analyzed with Eq.1. This provided space- and time-resolved information on LM thickness, as this was being periodically perturbed by a platform shaker oscillating by ±10 mm at 0-3.3 Hz. The introduction of these flows was important because LM walls will flow in a reactor, and be subject to secondary flows due to instabilities, turbulence and other effects[10–14]. The method presented is general with respect to the type of flow.

The only issue was that currents had to cross thick, short pieces of a good conductor (Galinstan). The resistances of interest were therefore small, the voltage signals were also small, and the signal-to-noise ratio relatively low. Still, despite noise, it was possible to achieve the desired precision of 1 mm and exceed the desired time-resolution (. . . instead of 10 ms), as illustrated by Fig.2. Higher precisions are obviously achievable for coarser time resolutions.

Note that, due to the finite width of the container, shallow liquid metal and large oscillatory motion, the surface waves excited in the LM were highly non-linear. Therefore, it was not surprising that, while periodic, the time-traces in Fig.2 were not pure sine-waves. Fast camera images confirmed the non-linear behavior and agreed on the existence of "steps" (Fig.2).

SUMMARY AND CONCLUSIONS

Resistive measurements of liquid metal thickness were spatially and temporally resolved for the first time. A theory was developed for $m \times n$ electrodes and experimentally demonstrated for 3×1 electrodes. Measurements were carried out with Galinstan in the absence of plasma, but are expected to succeed also with Lithium, whose conductivity is nearly identical.

Future work will be carried out in the presence of plasma. The diagnostic of thickness might require information from flowmeters and magnetics, due to complications associated with error fields and rapid flows, theoretically discussed in Sec.III.

[1]R. Majeski *et al.*, *J. Nuclear Materials* **313**, 625 (2003)
[2]R. Majeski *et al.*, *Nucl. Fusion* **45**, 519 (2005)
[3]R. Kaita *et al.*, *Phys. Plasmas* **14**, 056111 (2007)
[4]R. Majeski *et al.*, *Fusion Eng. Design* **85**, 1283 (2010)
[5]R.W. Moir, *Nucl. Fusion* **37**, 557 (1997)
[6]M.A. Abdou *et al.*, *Fusion Eng. Design* **54**, 181 (2001)
[7]F.L. Tabares, *Plasma Phys. Control. Fusion* **58**, 014014 (2015)
[8]R. Kaita *et al.*, *Rev. Sci. Instrum.* **72**, 915 (2001)
[9]R. Majeski *et al.*, *Phys. Plasmas* **20**, 056103 (2013)
[10]M. Narula *et al.*, *Fus. Eng. Design* **81**, 1543 (2006)
[11]N.B. Morley, M.S. Tillack, *Magnetohydrodynamics* **2**, 69 (1993)
[12]M.A. Jaworski *et al.*, *J. Nucl. Materials* **415**, S985 (2011)
[13]H. Ait Abderrahmane, G.H. Vatistas, *Fusion Eng. Design* **83**, 661 (2008)
[14]S.M.H. Mirhoseini, F.A. Volpe, *Plasma Phys. Control. Fusion*, submitted (2016), arXiv:1604.07473